

Natural ageing in magnesium alloys and alloying with Ti

Joka Buha

Received: 6 August 2007 / Accepted: 23 October 2007 / Published online: 3 December 2007
© Springer Science+Business Media, LLC 2007

Abstract This article reports on a remarkable natural ageing response observed for the first time in this work in Mg–Zn-based alloys. In these alloys, hardness in the naturally aged condition, generally, almost equals that in the artificially aged condition. The time to maximal hardness in the naturally aged condition can be dramatically reduced from several months needed for a binary Mg–Zn alloy, to a practical duration of a few weeks when some additional alloying elements that act as accelerants are added. Examples of such elements presented here are Cu and Ti. Strengthening in the naturally aged condition of these alloys is achieved through the formation of a very high density of Guinier-Preston (GP) zone-type precipitates. Both Cu and Ti also enhance the artificial ageing response by increasing the number density of the strengthening precipitates. Unlike Cu, Ti is not detrimental to the corrosion resistance and the current results indicate that it also has a very pronounced grain-refining effect on the Mg–Zn-based alloys.

Introduction

Magnesium alloys offer 30% weight reduction compared to aluminium alloys and 75% compared to steel, which makes them promising candidates for the light-weight applications in transportation systems. However, their mechanical properties are still inferior to those of the currently used aluminium alloys. Many magnesium alloys undergo precipitation hardening; however, the number density of the

precipitates formed during ageing is several orders of magnitude lower than in the precipitation hardenable aluminium alloys. Such widely spaced and often coarse precipitates are easily bypassed by gliding dislocations and provide limited strengthening. Increasing the number density of the precipitates and reducing the inter-particle spacing are therefore some of the main objectives of studies on precipitation hardening in magnesium alloys. Generally, this can be achieved through an appropriate alloying, appropriate thermo-mechanical treatment or by the combination of the two.

A notable fraction of the currently available cast and wrought magnesium alloys are based on the Mg–Zn system. These precipitation hardenable alloys are generally subjected to an artificial ageing heat treatment (T6), typically at temperatures between about 150 °C and 300 °C. Optimal strengthening in the T6 condition of Mg–Zn-based alloys is achieved mainly through the formation of the rod-like β'_1 precipitates perpendicular to the basal plane of magnesium [1, 2] due to their number density and orientation. The β'_1 rods are the predominant type of precipitate forming in the peak aged T6 condition of these alloys. A smaller fraction of β'_2 phase in the form of coarse plates parallel to the basal plane [1], or even laths perpendicular to the basal plane [3], may be present in this condition, along with the so-called blocky precipitates recently proposed to be a variant of the β'_1 phase [3]. The number density of the strengthening precipitates in a binary Mg–Zn alloy is generally very low and the precipitates are inhomogeneously distributed [2].

One of the alloying elements that increases the number density of the precipitates in Mg–Zn alloys and the homogeneity of their distribution, is Cu (ZC series of alloys) [1, 4, 5]. The Mg–Zn–Cu-based alloys are low-cost cast and wrought alloys known for their good mechanical properties;

J. Buha (✉)
National Institute for Materials Science, 1-2-1 Sengen,
Tsukuba 305-0047, Japan
e-mail: jokabuha@yahoo.com

however, the detrimental effect of Cu on the corrosion properties has been a challenge for their application. Another way of increasing the number density of precipitates is by conducting the ageing at reduced temperature, which generally increases the number of precipitate nuclei formed, and reduces the critical nucleus size. Reduced temperature ageing, including that at ambient temperature, is commonly observed in aluminium alloys; however, in most cases either the kinetics of the precipitation is very slow, or the size, morphology and type of the precipitates formed are inadequate for appreciable strengthening. Low-temperature ageing of magnesium alloys has been rarely studied. Earlier work on Mg–Zn alloy reported almost no increase in hardness during ambient temperature ageing for about 1000 h [6] and it has been assumed that magnesium alloys do not show any significant response to natural ageing. Very limited studies were performed on ageing at temperatures slightly above the ambient temperature but below the common T6 ageing temperature. Takahashi et al. [7], based on their X-ray diffraction studies on Mg–3.6 wt.%Zn alloy, reported on the formation of GP1 zones during ageing below 60 °C in the form of plates parallel to $\{11\bar{2}0\}_{\text{Mg}}$ planes, and GP2 zones below 80 °C in the form of oblate spheroids on $\{0001\}_{\text{Mg}}$ planes. These precipitates have not been characterized or even clearly observed by transmission electron microscopy (TEM). An additional type of disc-like GP zones has also been reported to form parallel to $\{0001\}_{\text{Mg}}$ planes [8].

This article reports for the first time on a remarkable natural ageing response in Mg–Zn-based alloys that results in the formation of significantly increased number density of fine precipitates when compared to the T6 condition. Ageing response to ambient temperature ageing is significantly accelerated in the presence of some additional alloying elements, such as Cu or Ti.

Table 1 Chemical composition of Mg–Zn–(Cu,Ti) alloys in wt.% and in at.% (given in brackets)

| Element, wt% (at%) | Mg | Zn | Cu | Ti | Mn |
|-----------------------|---------|---------|------------|-----------|------------|
| Mg–Zn | Balance | 7 (2.8) | <0.01 | – | <0.01 |
| Mg–Zn–Cu–Mn | | 6 (2.4) | 3 (1.2) | – | 0.1 (0.04) |
| Mg–Zn–Cu | | 4.6 (2) | 0.4 (0.15) | – | <0.01 |
| Mg–Zn–Ti | | 6 (2.4) | – | 0.8 (0.4) | <0.01 |

Table 2 Heat treatment schedules

| Alloy | Homogenisation | Solution treatment | | Ageing |
|-------------|----------------|--------------------|------------|-------------------------------|
| Mg–Zn | 335 °C-96 h | Cold water quench | 340 °C-5 h | Cold water quench T6 (160 °C) |
| Mg–Zn–Cu–Mn | 440 °C-48 h | | 440 °C-5 h | T4 (RT) |
| Mg–Zn–Cu | 435 °C-48 h | | 435 °C-5 h | |
| Mg–Zn–Ti | 340 °C-24 h | | 340 °C-4 h | |

Experimental procedures

Alloys of the compositions given in Table 1 were prepared from pure components by induction melting under protective Ar atmosphere and then cast into a permanent mould. Alloy ingots were then homogenized, solution heat treated and aged in an oil bath at 160 °C (T6) and in the air at room temperature (T4), as described in Table 2.

Vickers microhardness measurements were made using a load of 50 g and the results reported here are averaged from 12 measurements. Specimens for the TEM observations were prepared from aged alloy specimens by electropolishing in a solution of 22.32 g $\text{Mg}(\text{ClO}_4)_2$ and 10.6 g LiCl in 1000 mL methanol and 200 ml 2-butoxiethanol at about –45 °C and 90 V. Conventional TEM observations were performed using Phillips CM200 microscope operated at 200 kV. The high-resolution TEM (HRTEM) observations were performed using FEI Tecnai G2 F30 microscope operated at 300 kV. Optical microscopy observations were performed on alloy specimens in the as-homogenized condition after revealing the grain boundaries by etching using etchant 8 (acetic-picral) [9]. Grain size of alloy specimens was estimated in accordance with the planimetric method described in the ASTM standard E 112-96 (2004), i.e. by inscribing a circle on a micrograph and counting the number of grains included within the area and those intersected by a circle. Five randomly selected fields for each alloy specimen were used for the analysis. The grain size was then expressed as an average number of grains per square millimetre (\bar{N}_A). Scanning electron microscopy energy dispersive spectroscopy (SEM EDS) analysis was performed using a JEOL JSM 5400 scanning electron microscope equipped with JEOL JED 2140 energy dispersive X-ray microanalyzer.

Results

Age-hardening response

Figure 1(a) compares hardening of the binary Mg–Zn alloy (diamonds) during T6 heat treatment at 160 °C (solid symbols), and T4 heat treatment (open symbols). Current results show for the first time that hardness during natural

ageing equals that in the artificially aged condition and that Mg–Zn-based alloys do exhibit a significant age-hardening response to ambient temperature ageing.

For the binary alloy, ageing time needed for the hardness in the T4 condition to equal or become comparable to that in the T6 condition was at least 8 months. However, when certain other alloying elements are present in addition to Zn, the time to peak hardness in the T4 condition can be significantly reduced to a few weeks only. Such accelerated age-hardening response to natural ageing was observed for the first time in the current work for the Cu-containing Mg–Zn alloys. The T6 and T4 hardness curves of Mg–6Zn–3Cu–0.1Mn alloy (similar in composition to the commercial ZC63 alloy) are shown in Fig. 1(b). The T4 hardness curve of the binary alloy is also included in Fig. 1(b) for a comparison. The addition of Cu to Mg–Zn alloys apart from significantly improving the age-hardening response during artificial ageing, as previously reported by King and Unsworth [4, 5] and by Lorimer [1], also promotes a significant hardening at ambient temperature and hardness comparable to that in the T6 condition (109 VHN) can be reached after about 7 weeks of ageing (104 VHN). An identical general ageing response was observed for a number of Mg–Zn–Cu-based alloys with varying contents of Zn and Cu and the maximal hardness reached in the T4 condition is generally retained for the duration of the experiment (i.e., since the end of year 2005). Addition of Cu to Mg–Zn alloy therefore dramatically accelerates the kinetics of precipitation during natural ageing. An overall higher solute level in the Cu-containing alloy (including the presence of Mn), than in the binary alloy, is reflected in the higher as-quenched hardness. The binary alloy on the other hand, showed almost negligible response to natural ageing for 7 weeks (4 VHN increase from the as-quenched condition), which is consistent with the previously reported results by Mima and Tanaka [6], while a more prominent hardening became noticeable only after about 5 months of ageing (Fig. 1a). Figure 1(b) shows that the same kind of rapid natural ageing is promoted even by a trace amount of Cu (0.15 at.%) and in the absence of Mn. The T4 hardness of the Mg–4.6Zn–0.4Cu alloy almost equalled that in the T6 condition only after 4 weeks.

In order to promote the same combination of an accelerated natural ageing response and improved artificial ageing response using an element which does not have a detrimental effect on the corrosion resistance of alloy, as Cu does, a small amount of Ti was added to a Mg–6Zn alloy. Figure 1(c) shows that the Ti addition significantly affects the age-hardening response although Ti has been thought of having extremely low and unknown solubility in Mg (possibly expressed in parts per million) [10]. It should be noted that due to such limited solubility of Ti in the

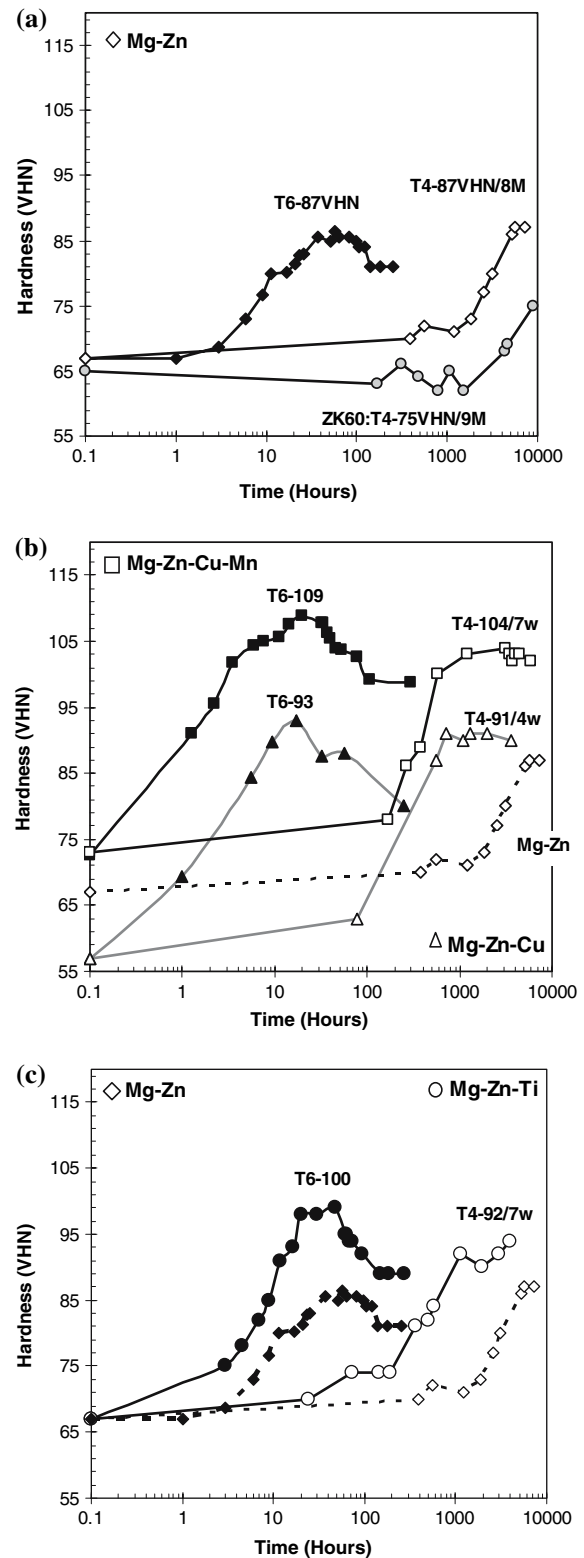


Fig. 1 T6 (solid symbols) and T4 (open symbols) hardness curves for alloys: (a) Mg–7Zn (diamonds) and ZK60 (grey circles-T4); (b) Mg–6Zn–3Cu–0.1Mn (squares), Mg–4.6Zn–0.4Cu (triangles) and Mg–7Zn (diamonds); and (c) Mg–6Zn–0.8Ti (circles) and Mg–7Zn (diamonds)

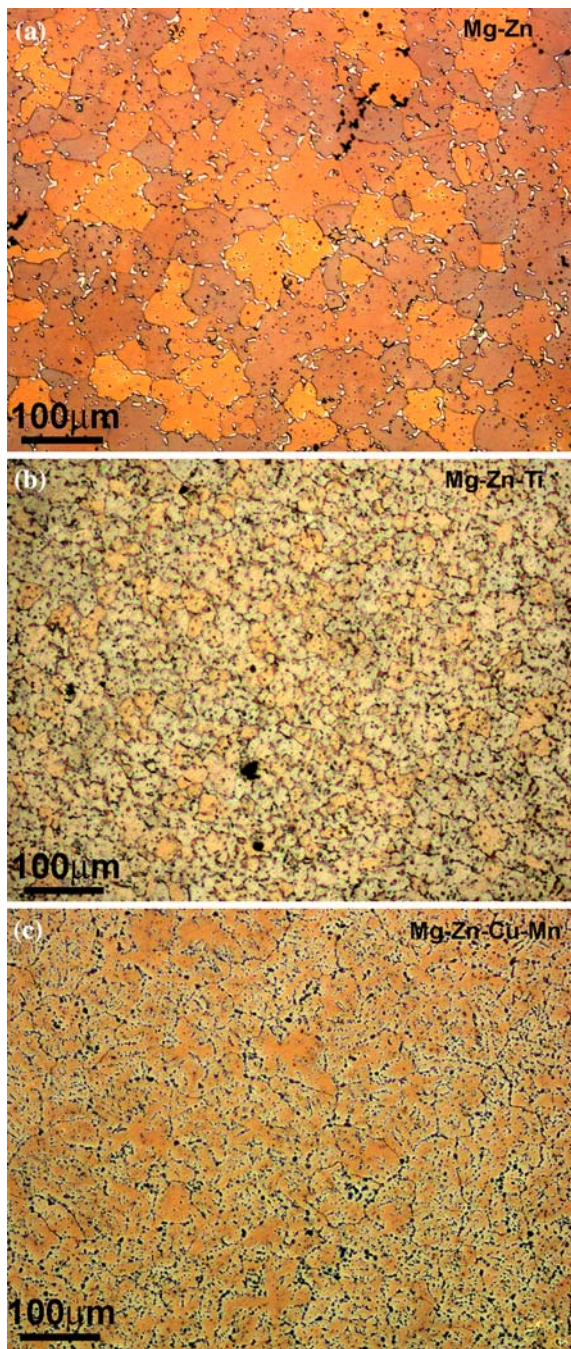


Fig. 2 Optical microscopy images of the as-homogenized microstructures of alloys: (a) Mg–7Zn; (b) Mg–6Zn–0.8Ti; and (c) Mg–6Zn–3Cu–0.1Mn

magnesium lattice, it is highly likely that an extremely small fraction of the total Ti added actually ended up in the solid solution, and thus became available to take part in the

precipitation. However, the presence of even a small amount of Ti in a Mg–Zn alloy significantly improves the age-hardening response during ageing at 160 °C and a higher hardness level is reached (100 VHN) for a shorter ageing time compared to the binary alloy. The onset of hardening after quenching is also shifted towards shorter ageing time; therefore, the kinetic of precipitation during artificial ageing is also significantly accelerated by the addition of Ti. Similarly to Cu, Ti also accelerates the remarkable hardening at ambient temperature, which becomes comparable to that produced during artificial ageing after less than 7 weeks of ageing.

Natural ageing response, in which the T4 hardness becomes almost equal to that in the T6 condition, appears to be common to Mg–Zn-based alloys. However, the time-to-peak in the T4 condition can vary considerably and it depends primarily on the type of other alloying elements present in addition to Zn. For example, presence of Zr in Mg–Zn alloy does not accelerate natural ageing, despite the fact that Zr has higher solubility in the magnesium lattice than Ti. Ageing response at ambient temperature of the commercial alloy ZK60 (composition close to Mg–4.7Zn–0.6Zr) quenched from 440 °C appears to be very similar to that of the binary Mg–Zn alloy (Fig. 1a, grey circles).

Grain-refining effect of Ti

Figure 2 compares the optical microscopy images from the as-homogenized alloys (a) Mg–7Zn, (b) Mg–6Zn–0.8Ti and (c) Mg–6Zn–3Cu–0.1Mn, after pical etch [9], which revealed the grain boundaries but also reacted with the grain boundary precipitates.

Simple visual comparison of these images shows that the Ti-containing alloy exhibited the smallest grain size. Quantitative analysis of the grain sizes, the results of which are presented in Table 3, also confirmed that for the Mg–Zn–Ti alloy the average number of grains per square millimetre was an order of magnitude higher than in the other alloys.

Using a SEM EDS analysis, precipitates visible on the grain boundaries of the binary alloy were determined to most likely be those of the eutectic Mg₇Zn₃ phase commonly observed in Mg–Zn alloys above the eutectoid temperature [11]. Precipitates visible in Mg–6Zn–3Cu–0.1Mn alloy have been referred to as the Mg(Zn,Cu)₂ eutectic phase in earlier works [1]; however, the exact

Table 3 Average number of grains per mm² (\bar{N}_A) of alloy specimens in the as-homogenized condition

| Alloy | Mg–7Zn | Mg–6Zn–3Cu–0.1Mn | Mg–4.6Zn–0.4Cu | Mg–6Zn–0.8Ti |
|--|---------------------|---------------------|---------------------|-----------------------|
| $\sim \bar{N}_A$ (grains/mm ²) (stdev) | 628 ⁽⁴³⁾ | 824 ⁽⁷⁹⁾ | 205 ⁽³⁰⁾ | 3011 ⁽⁷⁸⁷⁾ |

structure and composition of these precipitates are still unknown. Precipitates observed in this work contained roughly about 49 at.%Mg, 32 at.%Zn, 20 at.%Cu and about 0.1 at.%Mn. Preliminary analysis of the precipitates in the Ti-containing alloy showed that most of the precipitates were Mg and Zn rich and on average contained about 73 at.%Mg and 25 at.%Zn with very little (not more than 0.1 at.%) or no Ti present. Since it is possible that fine particles of pure Ti may also be present in the microstructure due to its very limited solubility in magnesium, a more detailed study is required to determine the exact origins of grain refinement in the Ti-containing alloy, which will be dealt with in a forthcoming publication.

Artificial ageing

Figure 3 compares the T6 peak-aged microstructures of the binary Mg–7Zn (c) alloy with that of the Mg–6Zn–3Cu–0.1Mn (b) and Mg–6Zn–0.8Ti (a) alloys. These TEM images show elongated rod-like precipitates of most likely the β'_1 phase perpendicular to magnesium basal plane as the predominant type of precipitate observed in all alloys. Inset images represent the selected area electron diffraction (SAED) patterns. In addition to β'_1 rods and a few coarse plates of most likely the β'_2 phase on basal planes, a smaller fraction of the precipitates similar to those recently described as blocky β'_1 [3], were also observed in all alloys, especially in the Ti-containing alloy. Similarly to earlier observations [2], the rod-like precipitates in the binary alloy in this study were generally coarse and inhomogeneously distributed. Apart from the known effect of Cu on increasing the number density of the β'_1 precipitates and making their distribution more homogeneous [1], current work shows that similar result can also be achieved by adding a very small amount of Ti. The number density of the precipitates was notably increased with the addition of Cu or Ti and it was generally higher in the presence of higher amounts of these elements. This indicates that both Cu and Ti stimulate the nucleation of precipitates during artificial ageing.

Natural ageing

Figure 4 shows the TEM images of the naturally aged microstructures of Mg–7Zn and Mg–6Zn–3Cu–0.1Mn alloys. In the binary alloy, naturally aged for 9 weeks, a very sparsely and inhomogeneously distributed prismatic

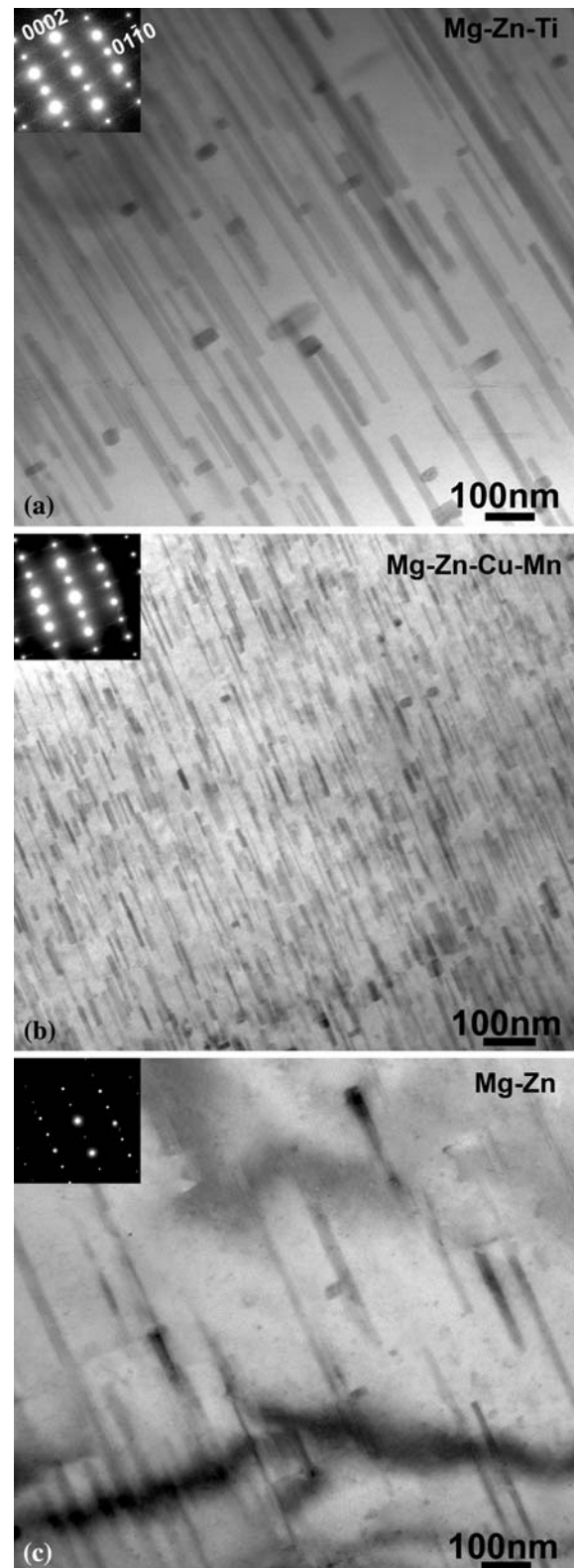


Fig. 3 $B//[2\bar{1}\bar{1}0]_{\text{Mg}}$ TEM images showing peak-aged T6 microstructures of alloys: (a) Mg–6Zn–0.8Ti; (b) Mg–6Zn–3Cu–0.1Mn; and (c) Mg–7Zn. Inset images are the corresponding SAED patterns

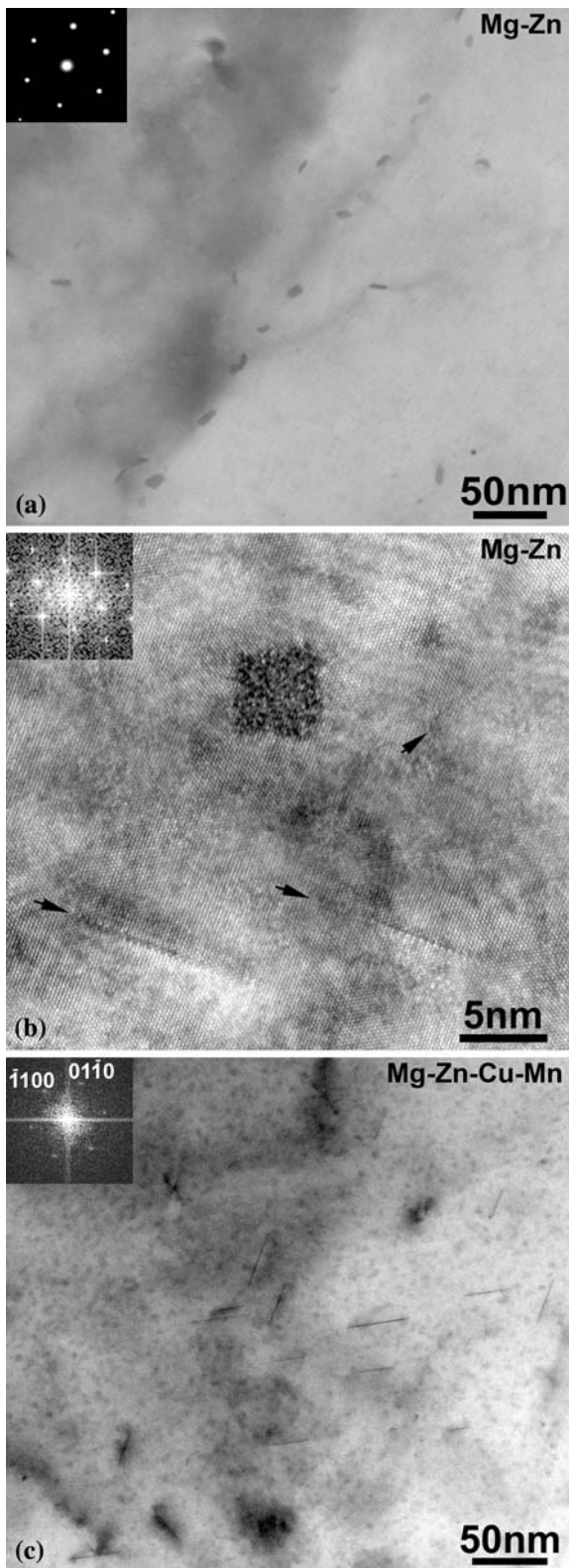


Fig. 4 B//[0001]_{Mg} (a) TEM and (b) HRTEM image of Mg–7Zn alloy naturally aged for 9 weeks; and (c) TEM image of alloy Mg–6Zn–3Cu–0.1Mn naturally aged for 8 weeks. Inset images in (b) and (c) are Fourier transforms (FFT) of the corresponding images

precipitates of an unknown phase were observed perpendicular to the basal planes of magnesium (Fig. 4a). The HRTEM image of one of these precipitates having a rectangular cross section is shown in Fig. 4(b). Such precipitates have not been observed before by TEM or HRTEM. It is uncertain whether these precipitates are in fact the GP2 zones detected earlier by Takahashi et al. [7]. In addition to these precipitates, the HRTEM observations with a [0001]_{Mg} electron beam direction also revealed very fine planar precipitates aligned with the $\langle 01\bar{1}0 \rangle_{\text{Mg}}$ directions (indicated in the fast Fourier transform (FFT) of the HRTEM image; indexed in Fig. 4c) thus lying on $\{2\bar{1}\bar{1}0\}_{\text{Mg}}$ planes (Fig. 4b). These precipitates correspond well to GP1 zones detected by Takahashi et al. [7]. Overall, the distribution of these precipitates was also very inhomogeneous. In the Cu-containing alloy on the other hand, a very high density of homogeneously distributed precipitates was observed after 8 weeks of natural ageing (Fig. 4c). Some of these precipitates were 20–50 nm in size planar precipitates on $\{2\bar{1}\bar{1}0\}_{\text{Mg}}$ planes, viewed edge-on in Fig. 4(c). The rest of the precipitates are visible as densely distributed mottled contrast using a conventional bright field TEM. This mottled contrast actually arises from the strain fields associated with even finer planar precipitates densely distributed on $\{2\bar{1}\bar{1}0\}_{\text{Mg}}$ planes, shown in the HRTEM image in Fig. 5(a), and with a smaller fraction of very fine prismatic precipitates (inset image in Fig. 5a). The fine planar precipitates are fully coherent with the magnesium lattice (Fig. 5a) and correspond well to GP1 zones, while the prismatic precipitates appear to be very similar to those observed in the binary alloy, although significantly smaller in size. Figure 5(b) shows a HRTEM image of the Cu-containing alloy taken from a $[01\bar{1}0]_{\text{Mg}}$ zone axis. From this direction one third of the planar GP1 zones, both fine and coarse, are again visible edge-on and clearly parallel to and coherent with $\{2\bar{1}\bar{1}0\}_{\text{Mg}}$ planes. The fine prismatic precipitates are not as clearly resolved and they are visible mostly as dark regions of approximately rectangular shape. The moiré fringes visible in Fig. 5(b) which have a wider spacing are associated with overlapping lattices of Mg and thin film of MgO formed on the surface of the specimen; however, those more closely spaced fringes which are also associated with the areas of dark contrast in the image are suspected to be a result of the presence of fine ordered prismatic precipitates. Figure 5(c) is a [0001]_{Mg} HRTEM image taken from the Mg–6Zn–0.8Ti alloy naturally aged for 8 weeks and it shows a high density of fine planar GP1 zones responsible for hardening observed in this alloy. Overall, the microstructures of the naturally aged Cu and Ti-containing alloys were very similar.

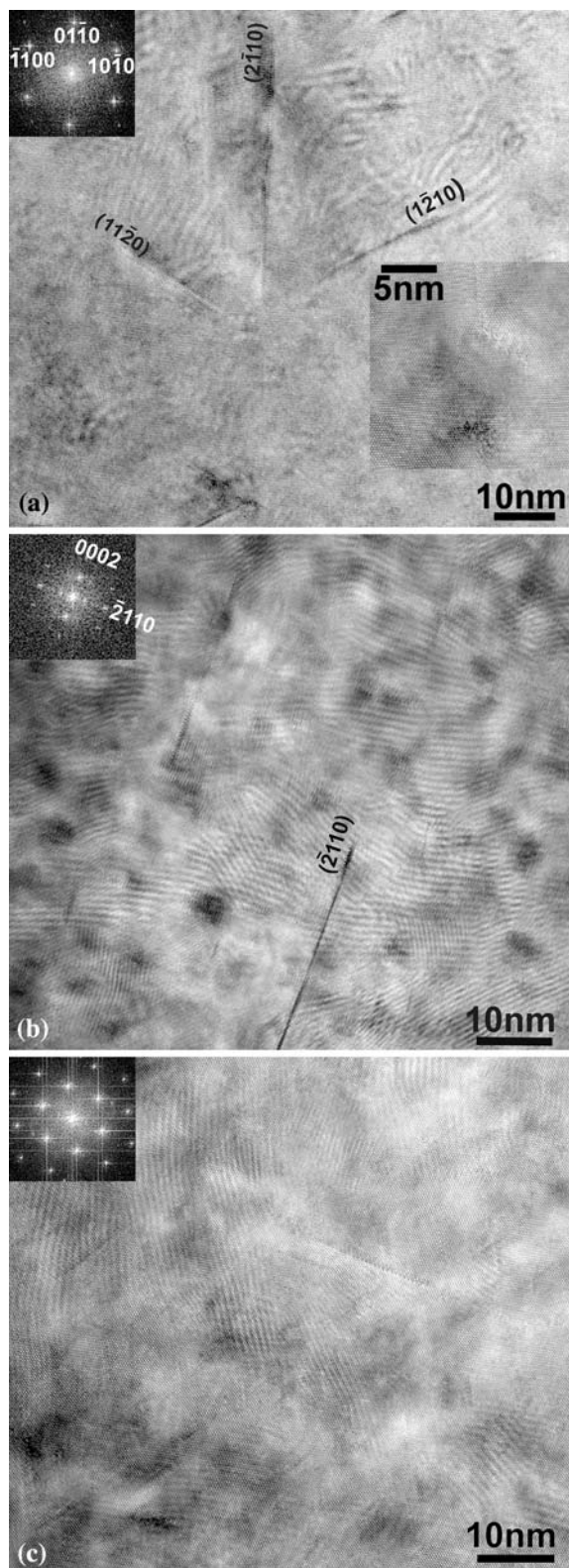


Fig. 5 (a) $B//[0001]_{\text{Mg}}$ and (b) $B//[01\bar{1}0]_{\text{Mg}}$ HRTEM images from naturally aged Mg–6Zn–3Cu–0.1Mn alloy; (c) $B//[0001]_{\text{Mg}}$ HRTEM image from naturally aged Mg–6Zn–0.8Ti alloy. Inset images represent the corresponding Fourier transforms (FFT) of the HRTEM images

Discussion

Magnesium alloys, in particular the Mg–Zn-based alloys, undergo a significant natural ageing following quenching from the solution heat treatment temperature. Due to the precipitation of a high density of very fine GP zone-type precipitates, hardness in the T4 condition can equal that in the T6 condition. The time needed for this may vary from several months (e.g. for binary Mg–Zn alloy and ZK60) to a few weeks in Mg–Zn–Cu and Mg–Zn–Ti alloys.

Hardness measurements and TEM observations presented here show that natural ageing phenomena in magnesium alloys allows for the formation of a very high density of closely spaced and coherent (GP1 zones) or semi-coherent (prismatic precipitates) precipitates that induce a considerable strain into the surrounding magnesium lattice. Such densely distributed and highly strained precipitates generally can not be by-passed by gliding dislocations. The interaction between the precipitates observed in the naturally aged condition of the Mg–Zn alloys containing Cu and Ti, and dislocations, most likely involves shearing, thus appreciable strength levels may be anticipated. A remarkable hardening in the T4 condition is promoted and accelerated by the addition of some elements, such as Cu and Ti. These elements promote the nucleation of precipitates and accelerate the kinetics of precipitation in Mg–Zn alloys. The nucleation of precipitates, their dispersion and the kinetics of precipitate nucleation and growth, are controlled by the distribution and concentration of vacancies [12–14]. The accelerated hardening effect during natural ageing and improved hardening effect during artificial ageing observed in the Cu-containing alloys may be partially ascribed to a higher solution treatment temperature of 440 °C (Table 2), thus higher vacancy supersaturation in the as-quenched condition than in the binary alloy (quenched from 340 °C). However, alloy-containing Ti shows the same remarkable natural ageing response when quenched from the same temperature as the binary alloy (and the total solute levels were also comparable). This indicates that the rapid natural ageing is not an effect of solely the higher solution heat treatment temperature, but more the effect of the type of alloying element added in the combination with Zn. This is confirmed also by the example of the Zr-containing commercial alloy ZK60 which does not show such accelerated natural ageing after being quenched from the same temperature as the Cu-containing alloy, and behaves as a simple binary alloy. Although Zr is primarily added for grain refining and not for improving the precipitation hardening, the solubility of Zr in magnesium lattice is significantly higher than that of Ti so a certain appreciable amount of Zr atoms is present in the solid solution, thus in a position to affect the nucleation of precipitates.

Therefore, some elements in the combination with Zn possibly promote the retention of vacancies in Mg alloys after quenching and by this ease the nucleation of the precipitates. From vast studies on aluminium alloys this is known to be one of the keys to manipulate the precipitation processes. Considering that the same rapid natural ageing response is achieved in two alloys (Mg–Zn–Cu and Mg–Zn–Ti) quenched from significantly different temperatures (440 °C and 340 °C) and therefore having different starting concentrations of vacancies (lower in the Mg–Zn–Ti alloy), it can be hypothesized that Ti (in the combination with Zn) may be even more effective in retaining the as-quenched vacancies and promoting the nucleation of precipitates than Cu. Current study demonstrates that the effect on natural ageing observed for Cu extends on other elements, and an example of Ti, which does not have a negative effect on the corrosion resistance of magnesium alloys, is presented in this article.

Conclusions

1. A significant natural ageing takes place in Mg–Zn-based alloys for which the hardness in the T4 condition generally almost equals that in the artificially aged T6 condition.
2. The time needed for the hardness in the T4 condition to reach that in the T6 condition can be reduced from several months (the case for the binary Mg–Zn alloy and the commercial Zr-containing alloy ZK60) to a few weeks (4–8 in general) when certain alloying elements, such as Cu or Ti, that act as accelerants of the precipitation processes are added.
3. Strengthening in the naturally aged condition is produced by the formation of a very high density of

mostly the fine planar GP1 zones and prismatic precipitates perpendicular to the basal plane of magnesium.

4. Addition of Ti to Mg–Zn alloy extensively improves the ageing response in general; it increases the number density of the precipitates in the T6 condition and promotes the remarkable and rapid natural ageing.
5. Addition of Ti also has a pronounced grain-refining effect on Mg–Zn alloy.

Acknowledgement The author wishes to acknowledge the financial support of the Japanese Society for the Promotion of Science (JSPS) in the form of a JSPS Postdoctoral Fellowship.

References

1. Lorimer GW (1986) Magnesium technology. Institute of Metals, London, p 47
2. Clark JB (1965) Acta Metall 13:1281
3. Gao X, Nie JF (2007) Scripta Mater 56:645
4. King JF, Unsworth W (1980) US Patent 4239535
5. Unsworth V (1987) Light Metal Age 8:10
6. Mima G, Tanaka Y (1971) Trans JIM 12:71
7. Takahashi T, Kojima Y, Takahashi K (1973) Jpn J Inst Light Metals 23:376
8. Polmear IJ (1995) Light alloys: metallurgy of the light metals, 3rd edn. Arnold, London, p 204
9. ASM Specialty Handbook (1998) Magnesium and magnesium alloys. ASM International, p 27
10. Hansen M (1958) Constitution of binary alloys, 2nd edn., written in cooperation with Anderko K. McGraw-Hill Book Co., New York, p 924
11. Wei LY, Dunlop GL, Westengen GL (1995) Metall Mater Trans A 26A:1947
12. Kelly A, Nicholson RB (1963) Prog Mater Sci 10:151
13. Lomer WM (1958) Inst Metals Monogr Rep Ser 23:79
14. Embury JD, Nicholson RB (1965) Acta Metall 13:403